Critical current measurements in superconductor-ferromagnet-superconductor junctions of YBa$_2$Cu$_3$O$_y$-SrRuO$_3$-YBa$_2$Cu$_3$O$_y$: No evidence for dominant proximity-induced triplet superconductivity in the ferromagnetic barrier

G. Koren,[*] T. Kirzhner, and P. Aronov

Physics Department, Technion-Israel Institute of Technology, 32000 Haifa, Israel
(Received 30 November 2011; revised manuscript received 26 December 2011; published 6 January 2012)

Transport measurements in ramp-type junctions of YBa$_2$Cu$_3$O$_y$-SrRuO$_3$-YBa$_2$Cu$_3$O$_y$ with T_c values of either 80–90 K or 60–70 K are reported. In both types of junctions but without a barrier ("shorts"), the supercurrent densities at 4.2 K reached 7.5 and 3.5 MA/cm^2, respectively, indicating the high quality of the fabrication process. Plots of the critical current versus thickness of the ferromagnetic barrier at 4.2 K show exponential decays with decay lengths of 1.1 nm for the 90-K phase and 1.4 nm for the 60-K phase, which are much shorter than the relevant coherence lengths $\xi_F \sim$ 5–6 nm or $\xi_N \sim$ 16 nm of SrRuO$_3$. We thus conclude that there is no dominant proximity induced triplet superconductivity in the ferromagnet in our junctions.

I. INTRODUCTION

In a recent feature article in the January 2011 issue of Physics Today, Matthias Eschrig reviews the rapidly growing field of proximity-induced triplet superconductivity (PITS) in ferromagnets in contact with a superconductor, which attracted much attention in the past few years.[1] In the present study, we did not observe this effect in superconductor-ferromagnet-superconductor (SFS) junctions of the high-temperature superconductor YBa$_2$Cu$_3$O$_y$ (YBCO) and the itinerant ferromagnet SrRuO$_3$ (SRO), and believe that this finding is due to the very narrow domain walls of SRO. Basically, standard singlet superconductivity and strong ferromagnetism are two antagonistic phenomena due to their different spin ordering configurations. It should therefore be hard to obtain supercurrents in SFS junctions when the barrier thickness d_F is much larger than the short coherence length of the ferromagnet, either $\xi_F = \hbar v_F / 2E_{ex}$ in the clean limit or $\xi_F = \sqrt{\hbar D / 2E_{ex}}$ in the dirty limit, which are affected mostly by the exchange energy $E_{ex} \sim k_B T_{\text{Curie}}$.[2,3] This, however, is not the case if the singlet pairs in S, in the vicinity of the SF interface, would induce equal-spin triplet pairs in the ferromagnet via the proximity effect. Then, due to the compatibility of the triplet and ferromagnetic orders, a supercurrent could be maintained at low temperature over a long range of $d_F \sim 2\xi_N$ with a coherence length $\xi_N = \sqrt{\hbar D / 2\pi k_B T}$ rather than the shorter ξ_F ones.

A number of theoretical studies had predicted the PITS effect, which can originate in interface inhomogeneities such as natural domain walls or artificial magnetic structures.[4–8] Supercurrents consistent with PITS theories were observed experimentally in SFS junctions with remarkably long half-metal ferromagnetic CrO$_2$ barriers ($d_F = 300$–700 nm) and low-T_c s-wave superconductors,[9,10] and in Nb-based SFS junctions with engineered multilayered ferromagnetic barriers.[11,12] Critical currents had also been observed in highly polarized La$_{2/3}$Sr$_{1/3}$MnO$_3$ (LSMO) barrier ($d_F = 20$ nm) and the high-T_c d-wave superconductor YBCO.[13] In the low-T_c junctions with multilayer barriers,[11,12] systematic measurements of the supercurrent were performed versus the ferromagnetic barrier thickness. In the present study we also report on such measurements in SFS ramp-type junctions of YBCO and SRO.

At 4.2 K, the critical current plots versus the barrier thickness show decay lengths ξ, which are much shorter than ξ_F thus excluding the possibility of a dominant PITS component in the ferromagnet in our junctions.

II. BASIC JUNCTION PROPERTIES

About 200 junctions on 20 wafers of (100) SrTiO$_3$ (STO) were prepared and characterized in the present study. For this, we fabricated ten ramp-type junctions on each wafer in the geometry shown in the inset to Fig. 1 by a multistep process, which included laser ablation deposition of the thin films, deep ultraviolet photolithographic patterning, and Ar ion milling.[14] The junctions generally had different SRO barrier thickness (d of 0, 4.5, 9, 13, 18, 22.5, and 45 nm) but the same YBCO electrodes' thickness (80 nm). They were fully epitaxial with the c axis normal to the wafer, coupled in the a-b planes between the base and cover electrodes and oriented along the (100) STO direction. They also had a ramp angle of about 35° with the wafer, 5 μm width, and their cross section area was 0.4 μm^2. The resulting junctions were generally annealed under 50 Torr of oxygen pressure to produce optimally doped electrodes of the 90-K YBCO phase. Some junctions, however, were re-annealed under oxygen flow of 0.1 Torr, which yielded the 60-K phase of YBCO. The SRO barrier has remained unchanged under these annealing conditions. This allowed us to test if our critical current results are sensitive to the doping of YBCO and in what way.

III. RESULTS AND DISCUSSION

A. Resistance versus temperature and I-V curves

Typical four-probe results of the resistance versus temperature of two junctions with $d = 4.5$ nm are shown in Fig. 1. In addition to the superconducting transition temperatures of the YBCO electrodes at 87–90 K, there are two weakly resistive tails of a few Ω down to 70 and 60 K where the junctions reach zero resistance. The top inset of this figure shows a current versus voltage (I-V) curve at 4.2 K of the junction with the lower normal resistance and $T_c(R = 0) = 70$ K (J5). One can see that the critical current (I_c) is of about 5.5 mA while the critical current density (J_c) is 1.4 MA/cm^2. The
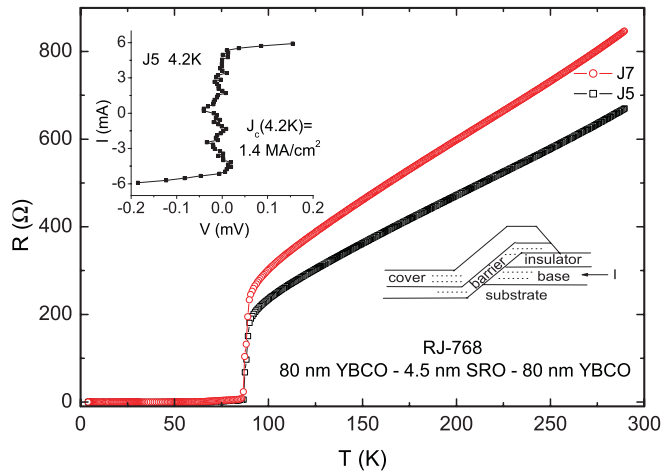
FIG. 1. (Color online) Resistance versus temperature of two YBCO/4.5-nm SRO/YBCO junctions with the I-V curve of J5 at 4.2 K in the top inset. The bottom inset shows a schematic drawing of a ramp-type junction, where the 80-nm-thick base and cover electrodes are made of YBCO and the barrier is made of SRO.

FIG. 2. (Color online) Resistance versus temperature of eight YBCO/9-nm SRO/YBCO junctions with the I-V curve of one of the junctions with zero resistance at 4.2 K (J1) shown in the inset.

noise near zero bias is due to bad contacts in this case, though generally gold coated contacts were used, which had much lower noise. The second junction (J7) with the higher normal resistance and lower $T_c(R = 0) = 60$ K, had about half of the supercurrent of the first junction. This strong variation in the supercurrents is typical of our junctions with the ferromagnetic SRO barrier, and this effect becomes even more pronounced with increasing barrier thickness. With the present small barrier thickness of 4.5 nm, however, we can not rule out the existence of microshorts due to the nanometer roughness of the two SF interfaces of the junctions,[15] and the possibly incomplete coverage of the base electrode with the thin SRO layer. For comparison we fabricated and tested "shorts," which are ramp-type junctions prepared by exactly the same process but without the barrier. These had at 4.2 K maximal J_c values of 7.5 and 3.5 MA/cm^2 for the junctions with $T_c \sim 80$–90 and $T_c \sim 60$–70 K, respectively. Thus the effect of possible microshorts in the junctions of Fig. 1 is not dominant, as their maximal supercurrent density is still a factor of about 5 (7.5/1.4) lower than that of the corresponding short.

Figure 2 shows the resistance versus temperature results of eight junctions with SRO barrier thickness of $d = 9$ nm and $T_c \sim 87$–90 K. The different normal-state resistances are due to different lengths of the leads to the junctions. Actually, J5 and J6 have similar lead lengths and therefore their normal resistances are quite similar. The same is true for J1 and J10, and also for J3 and J8. Figure 2 clearly shows the wide spread of the junctions' resistance below T_c of the electrodes. This effect has been observed before[16] and was attributed to the nonuniform interface resistance whose origin is still unclear. In the present study, however, we shall not focus on the highly resistive junctions, but on those with lowest resistance which generally have the highest supercurrents. A typical I-V curve at 4.2 K of one of the junctions with zero resistance (J1) is shown in the inset to Fig. 2. One can see that the junction becomes slightly resistive with a resistance of a few Ω at a relatively low bias. This generally depends on earlier magnetic-field exposure or history of the junction
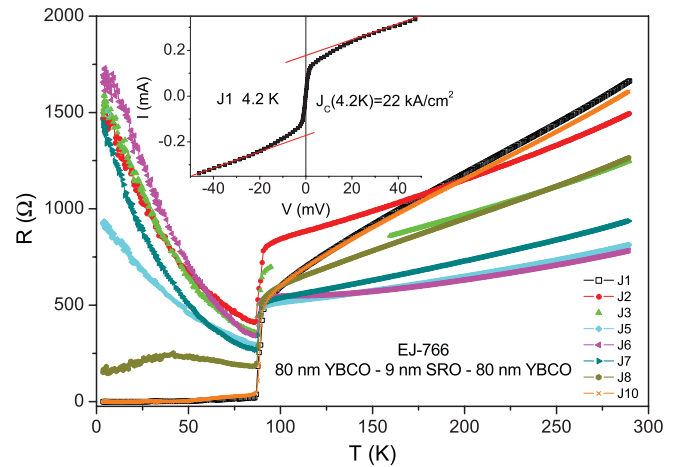
(trapped flux), or on the intrinsic magnetic field emanating from the ferromagnetic barrier. Both of these effects lead to flux creep resistance with increasing bias. At higher bias, the critical current is reached and a change to the normal state is observed where the rounding is now due to flux flow and also to thermal noise. The high bias slope of the I-V curve yields a normal resistance R_N of $\sim$300 Ω, which is much higher than that calculated from the SRO resistivity and junction geometry (about 10 mΩ). This result therefore originates in the the two interfaces of the junctions as has already been observed before.[16] We generally determine the I_c values of the junctions by extrapolating the high bias data to zero bias as shown in the inset to Fig. 2. At 4.2 K this yields a J_c value of 22 kA/cm^2 for junction J1 of Fig. 2. Junction J10 had comparable supercurrent density, while the other junctions had much smaller critical currents or none at all. We therefore decided that for comparison between junctions with different barrier thickness we shall always take the maximal I_c values of one or two junctions on each wafer.

The main panel of Fig. 3 presents I-V curves with a resistively shunted junction (RSJ) behavior at 4.2 K of a junction with an SRO barrier thickness of 13 nm and T_c in the range 85–89 K. The critical current can be determined by the use of the RSJ formula given in this figure, or by the extrapolation procedure as shown before in the inset to Fig. 2. The extrapolation procedure, however, underestimates the supercurrent in this case and we therefore chose to use the I_c values derived from the RSJ formula. Also shown in this figure are I-V curves under magnetic fields of 1 and 3 T, where the I_c values are suppressed, the flux flow resistance increases, and the RSJ behavior is almost washed out. The inset to Fig. 3 shows two oscilloscope traces of I-V curves with a zoom up on the low bias regime. These were measured on a junction with the same barrier thickness of 13 nm but on a different wafer that had T_c values in the range 64–70 K. Under microwave radiation, the junction became resistive at zero bias with a resistance of a few ohms. Unlike the dc measured results of the main panel, which generally took 1–2 min. to record, the ac measured results in the inset were obtained with an averaging digital oscilloscope and took about 1 s. In the ac
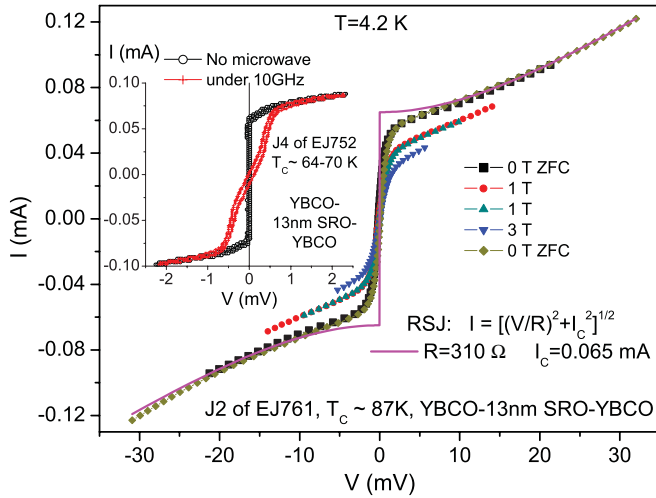
FIG. 3. (Color online) Current versus voltage curves at 4.2 K of an YBCO/13-nm SRO/YBCO junction with RSJ behavior, under zero field cooling (ZFC) and under 1 and 3 T magnetic fields. The solid curve is an RSJ fit with the formula and parameters given in the figure. The inset shows two oscilloscope traces of I-V curves at 4.2 K near zero bias with and without 10 GHz microwave radiation, on a similar junction but on a different wafer with $T_c \sim 67$ K.

case, except for some hysteresis, no flux creep resistance could be observed up to the critical current at about 0.072 mA, which is comparable to the result of the main panel. Since flux creep is more probable in the dc measurements than in the ac ones due to the longer time available for depinning, this leads to the observed small flux creep resistance at low bias in the main panel, which is absent in the inset. We note that the I-V curve without microwave radiation in the inset of Fig. 3 is similar to those obtained in Ref. 17 on similar junctions, although the normal resistance here is much larger ($\sim$100 Ω).

Figure 4 shows I-V curves at 4.2 K of underdoped junctions with $T_c \sim 60$–70 K and 18 nm SRO barrier thickness on three different wafers. The spread of the maximal I_c values here is quite large and ranges between 7 and 60 μA. The low bias
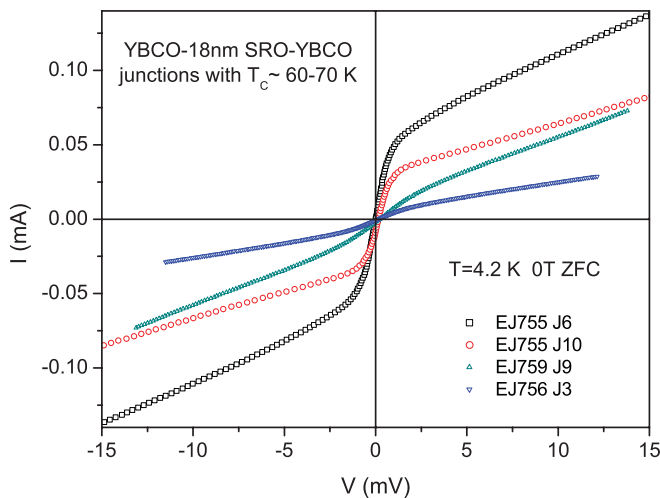
FIG. 4. (Color online) Current versus voltage curves at 4.2 K of four YBCO/18-nm SRO/YBCO junctions with $T_c \sim 60$–70 K and with the highest I_c values on three wafers.

resistance due to flux flow is quite pronounced and it seems hard to distinguish between a critical current and a zero-bias conductance peak (ZBCP) due to bound states. ZBCPs were observed before in the same kind of SFS and SF junctions.[16,18] In SF junctions, however, where no supercurrent exists, the normalized ZBCP are small, typically up to 0.1. Since the normalized conductances dI/dV at zero bias in Fig. 4 here range between 3 and 20, we conclude that the apparent ZBCP contribution to the critical current is negligible.

B. Critical current dependence on the barrier thickness

Figure 5 presents the main result of the present study. It shows all the maximal measured I_c values of one or two junctions on each wafer as a function of the SRO barrier thickness. It also shows which data point belongs to the 80–90-K phase and which to the 60–70-K phase of YBCO. No critical current could be found in the junctions with the 45-nm-thick barrier. The three exponential decay fits of the data correspond to all data points, and to the two different YBCO phases separately. We stress that due to the two SF interfaces in each SFS junction, the decay length is 2ξ rather than ξ. Since our procedure of taking the maximal critical currents of one or two junctions on each wafer is nonstandard, we show for comparison in Fig. 6 the critical current results of all working junctions with $T_c \sim 60$–70 K as a function of the SRO barrier thickness, together with the corresponding exponential decay fit. The data now are clearly much more scattered, but the exponential decay length $\xi = 1.3$ nm is almost the same as in Fig. 5 (1.4 nm for the phase with $T_c \sim 60$–70 K). The large error range of ξ in Fig. 6 (± 2 nm) reflects the fact that in junctions with a large barrier thickness the spread of the data is much larger than in those with a small one. Thus the fact that almost the same value of ξ results from the data of both Figs. 5 and 6 justifies the way we chose to present the data in Fig. 5.
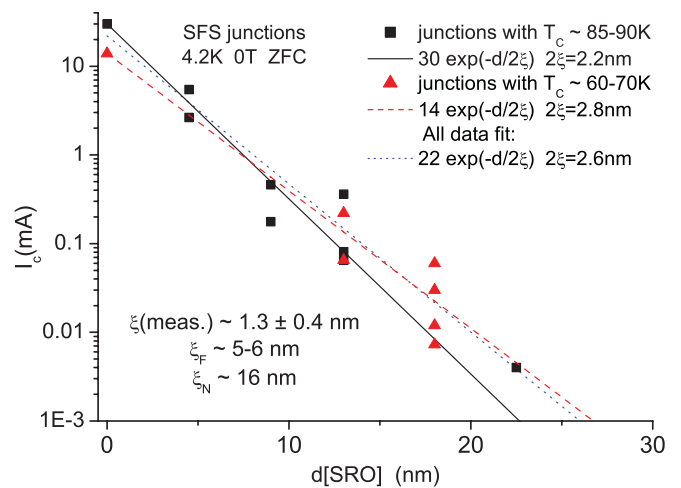
FIG. 5. (Color online) Maximal critical current values at 4.2 K of one or two junctions on each wafer as a function of the SRO barrier thickness. Data are shown for the junctions with $T_c \sim 80$–90 K and the junctions with $T_c \sim 60$–70 K. The corresponding exponential decay fits are given by the solid and dashed lines, respectively, together with a fit of all the data (dotted line).
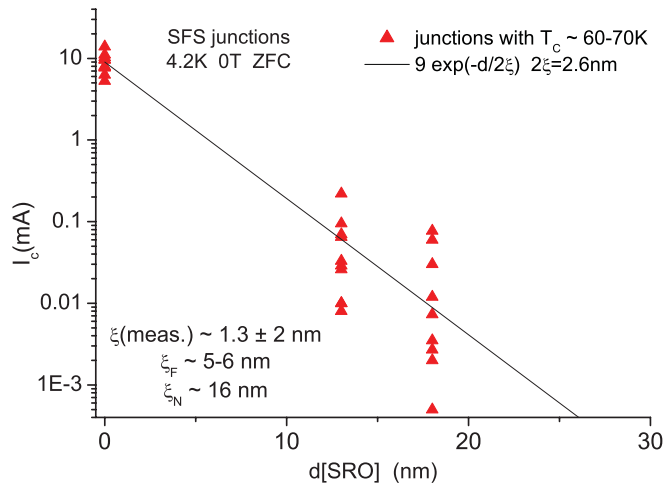
FIG. 6. (Color online) Critical current values at 4.2 K of all working junctions with $T_c \sim 60$–70 K as a function of the SRO barrier thickness, together with an exponential decay fit. The resulting ξ value is almost the same as in Fig. 5, but the error range now is much larger.

The immediate clear result from the fits of Fig. 5 is that all three decay lengths $\xi = 1.1$, 1.3, and 1.4 nm are significantly shorter than ξ_F of SRO, which is either about 4.8 nm in the clean limit where $\xi_F = \hbar v_F / 2E_{ex}$, or about 6.2 nm in the dirty limit where $\xi_F = \sqrt{\hbar D / 2 E_{ex}}$. These values were obtained using a Fermi velocity $v_F \sim 2 \times 10^5$ ms^{-1} and a mean free path at 4 K of $\ell \sim 14$ nm,[19,20] with the diffusion coefficient $D = v_F \ell / 3$. For the exchange energy we used $E_{ex} \sim k_B T_{Curie} \sim 13$ meV, which is quite close to the $\sim$10-meV value obtained from Faraday rotation measurements.[21] The latter though depends on subtraction of a large phonon contribution, so we used the former. Our measured 2ξ values of 2.2–2.8 nm can be qualitatively compared with those obtained in Ref. 17, where mixed data of J_c in junctions with SRO as well as CaRuO$_3$ barriers yield $2\xi = 6.2$ nm. This larger value is apparently affected also by the low J_c at $d_F = 0$ (short) in their study, which is smaller by a factor of $\sim$20 than in the present work. If a significant amount of equal-spin triplet pairs are induced in the ferromagnetic SRO barrier, we should have actually had to compare the measured ξ values with ξ_N of SRO. In SRO films with normal c-axis orientation, the domain walls are in the (110) direction and their spacing is of about 1000 nm.[22] Thus in the present (100) oriented junctions with up to 45-nm-thick barriers, transport occurs mostly via single domains with very little scattering at domain walls. In this case, one obtains $\xi_N = \sqrt{\hbar D / 2\pi k_B T} \sim 16$ nm in the dirty limit of SRO, which is obviously much larger than either of the ξ_F values given above. We thus conclude that in the present SFS junctions, no significant PITS affects the measured critical currents.

Finally, we shall check the present result in the context of previous results on the YBCO-SRO system.[16,18,23] The scanning tunneling spectroscopy results of SRO/(100)YBCO bilayers show a long-range penetration of the superconducting order parameter via the SRO layer up to $d_F = 26$ nm,[23] but only along lines that are correlated with the magnetic domain-wall structure of the ferromagnet. In SFS and SF junctions, ZBCPs were found whose zero-field magnitude also correlated with the number of domain walls in the SRO barrier.[16,18] Both results were interpreted as due to nonlocal crossed Andreev reflection effect (CARE) near domain walls crossing the interface, but could also be partially attributed to PITS. Due to the small fraction of the junction cross section area where these effects can occur ($\xi_S \times d_F \times N$ where $\xi_S \sim 2$ nm is the coherence length of YBCO, d_F is the SRO layer thickness, and N is the number of domain walls crossing the interfaces in the junctions), their total contribution to the critical current is apparently small. Therefore the present critical current results with the very short ξ values can be explained as due to dominant local Andreev reflections that are present in the partially spin-polarized SRO barrier [$P \sim 50\%$ at 4.2 K (Ref. 24)]. We plan to check in the near future the critical currents of YBCO-La$_{2/3}$Ca$_{1/3}$MnO$_3$-YBCO junctions, where the polarization of the manganite is almost 100% and the domain walls are much broader. We expect that in these junctions, a more dominant contribution to the critical current by PITS will be observed. Alternatively, as was done recently in conventional low-T_c SFS junctions,[11,12] artificial engineering of the ferromagnetic barrier in YBCO-SRO-YBCO junctions could introduce sufficiently large inhomogeneity to allow for a more prominent PITS contribution to the supercurrents to be observed.

IV. CONCLUSIONS

Very short decay lengths of the critical current on the order of 1–2 nm were observed in the ferromagnetic barrier of YBCO-SRO-YBCO junctions, which are much shorter than the corresponding penetration lengths ξ_F and ξ_N of SRO. This result is attributed to the absence of a dominant proximity induced triplet superconductivity in the SRO layer in the present junctions. It was also found that the degree of interface inhomogeneity originated by the domain walls of the ferromagnet is key for the understanding of the present observation.

*gkoren@physics.technion.ac.il;

http://physics.technion.ac.il/~gkoren

[1] M. Eschrig, Phys. Today **64**(1), 43 (2011).

[2] F. S. Bergeret, A. F. Volkov, and K. B. Efetov, Rev. Mod. Phys. **77**, 1321 (2005).

[3] A. I. Buzdin, Rev. Mod. Phys. **77**, 935 (2005).

[4] F. S. Bergeret, A. F. Volkov, and K. B. Efetov, Phys. Rev. Lett. **86**, 4096 (2001).

[5] Ya. V. Fominov, A. F. Volkov, and K. B. Efetov, Phys. Rev. B **75**, 104509 (2007).

[6]M. Eschrig and T. Lofwander, Nat. Phys. **4**, 138 (2008).

[7]Joern N. Kupferschmidt and Piet W. Brouwer, Phys. Rev. B **80**, 214537 (2009).

[8]A. F. Volkov and K. B. Efetov, Phys. Rev. Lett. **102**, 077002 (2009).

[9]R. S. Keizer, S. T. B. Goennenwein, T. M. Klapwijk, G. Miao, G. Xiao, and A. Gupta, Nature (London) **439**, 845 (2006).

[10]M. S. Anwar, F. Czeschka, M. Hesselberth, M. Porcu, and J. Aarts, Phys. Rev. B **82**, 100501(R) (2010).

[11]Trupti S. Khaire, Mazin A. Khasawneh, W. P. Pratt Jr., and Norman O. Birge, Phys. Rev. Lett. **104**, 137002 (2010).

[12]J. W. A. Robinson, J. D. S. Witt, and M. G. Blamire, Science **329**, 59 (2010).

[13]M. Q. Huang, Z. G. Ivanov, P. V. Komissinski, and T. Claeson, Physica C **326-327**, 79 (1999).

[14]O. Nesher and G. Koren, Appl. Phys. Lett. **74**, 3392 (1999); Phys. Rev. B **60**, 9287 (1999); **60**, 14893 (1999).

[15]G. Koren and N. Levy, Europhys. Lett. **59**, 121 (2002); **59**, 634(E) (2002).

[16]P. Aronov and G. Koren, Phys. Rev. B **72**, 184515 (2005).

[17]L. Antognazza, K. Char, T. H. Geballe, L. L. King, and A. W. Sleight, Appl. Phys. Lett. **63**, 1005 (1993).

[18]T. Kirzhner and G. Koren, Phys. Rev. B **82**, 134507 (2010).

[19]P. B. Allen, H. Berger, O. Chauvet, L. Forro, T. Jarlborg, A. Junod, B. Revaz, and G. Santi, Phys. Rev. B **53**, 4393 (1996).

[20]G. Santi and T. Jarlborg, J. Phys.: Condens. Matter **9**, 9563 (1997).

[21]J. S. Dodge, E. Kulatov, L. Klein, Ch. H. Ahn, J. W. Reiner, L. Mieville, T. H. Geballe, M. R. Beasley, A. Kapitulnik, H. Ohta, Y. Uspenskii, and S. Halilov, Phys. Rev. B **60**, R6987 (1999).

[22]A. F. Marshall, L. Klein, J. S. Dodge, C. H. Ahn, J. W. Reiner, L. Mieville, L. Antogonazza, A. Kapitulnik, T. H. Geballe, and M. R. Beasley, J. Appl. Phys. **85**, 4131 (1999).

[23]I. Asulin, O. Yuli, G. Koren, and O. Millo, Phys. Rev. B **74**, 092501 (2006).

[24]P. Raychaudhuri, A. P. Mackenzie, J. W. Reiner, and M. R. Beasley, Phys. Rev. B **67**, 020411(R) (2003).